



University of
New Haven

University of New Haven
Digital Commons @ New Haven

Civil Engineering Faculty Publications

Civil Engineering

1-2017

Freeze-thaw Durability of Concrete Columns Wrapped with FRP and Subject to Corrosion-Like Expansion

Ronald S. Harichandran

University of New Haven, rharichandran@newhaven.edu

M.I. Baiyasi

Elsinore Valley Municipal Water District

G. Nossioni

Manhattan College

Follow this and additional works at: <http://digitalcommons.newhaven.edu/civilengineering-facpubs>

 Part of the [Civil Engineering Commons](#)

Publisher Citation

Harichandran, R. S., Baiyasi, M. I., and Nossioni, G. (2016). "Freeze-thaw durability of concrete columns wrapped with FRP and subject to corrosion-like expansion." *Journal of Materials in Civil Engineering*, 29(1).

Comments

This is the authors' accepted manuscript of the article published in *Journal of Materials in Civil Engineering*. The version of record can be found at [http://dx.doi.org/10.1061/\(ASCE\)MT.1943-5533.0001691#sthash.JA9OUibt.dpuf](http://dx.doi.org/10.1061/(ASCE)MT.1943-5533.0001691#sthash.JA9OUibt.dpuf)

1
2
3 **FREEZE-THAW DURABILITY OF CONCRETE COLUMNS WRAPPED**
4 **WITH FRP AND SUBJECT TO CORROSION-LIKE EXPANSION**
5

6 R. S. Harichandran,¹ M. I. Baiyasi² and G. Nossoni³
7

8 **ABSTRACT**

9 Experiments were conducted to assess the effects of using fiber-reinforced polymer (FRP)
10 wraps, with fibers oriented in the hoop direction, for rehabilitating corrosion-damaged
11 columns. This paper reports findings related to the freeze-thaw durability of concrete
12 specimens with round and square cross sections, wrapped with glass and carbon FRP, after
13 they are subjected to an internal expansive force similar to that generated by corroding steel.
14 The results of the experiment indicate that freeze-thaw cycles have no statistically significant
15 effect on the compressive strength of glass and carbon wrapped specimens. Freeze-thaw
16 conditioning generally reduced the longitudinal failure strain of wrapped specimens. The
17 square wrapped specimens had lower compressive strength compared to the round
18 specimens, even though the cross sectional area of the square prisms was higher than that of
19 the round cylinders. This is due to the reduced confinement provided by the wraps for square
20 cross sections and stress concentrations that develop at the corners. Wrapped square prisms
21 always failed by rupture of the wrap at a corner. A reduction of approximately 30% to 40%

¹ Dean, Tagliatela College of Engineering, University of New Haven, West Haven, CT 06516.

² Manager, Elsinore Valley Municipal Water District, 31315 Chaney St, Lake Elsinore, CA 92530

³ Asst. Prof., Department of Civil and Environmental Engineering, Manhattan College, Riverdale, NY 10471.

22 in failure stress was noted between wrapped specimens with round and square cross sections,
23 respectively.

24

25

INTRODUCTION

26 One of the main causes of deterioration in reinforced concrete structures is corrosion
27 of the reinforcement bars (Du et al. 2006). The strength, durability and service life of
28 concrete structures are reduced by corrosion. Corrosion products can have a volume of up to
29 600% of the original volume of the corroding steel (Mehta and Monteiro 1993). This extra
30 volume applies pressure to the surrounding concrete and causes cracking and delamination of
31 the concrete cover. Both oxygen and chloride is required for the corrosion activity to start. If
32 a barrier reduces the diffusion of oxygen and chloride into concrete, then the time to
33 corrosion will reduce considerably. Using FRP wraps is one way to introduce a barrier that
34 retards the diffusion of oxygen and chloride into concrete, thereby increasing the service life
35 and durability of concrete structures (Nossoni 2015).

36 FRP materials have been used over the past two decades in civil engineering
37 structures for different strengthening applications because of their superior mechanical
38 properties as well as their resistance to aggressive environmental conditions. However, some
39 environmental factors such as extreme temperature fluctuation and water absorption can
40 adversely affect the behavior of some polymer composite material. Water absorption reduces
41 the strength and stiffness of some polymeric composites by as much as 30% compared to dry
42 material. Water absorption can break down the interface between the reinforcing fiber and
43 resin matrix leading to loss of strength and rigidity. Cycles of freezing and thawing tend to
44 magnify the effect of water absorption (Gomez and Casto 1996).

45 While several studies have been conducted on the strength of columns wrapped with
46 FRPs, studies on durability under harsh environmental conditions such as freeze-thaw and
47 exposure to chloride are much fewer (Soudki 1997, Toutanji and Balaguru 1998, Rivera and
48 Karbhari 1999, Almusallam et al. 2000, El-Zefzafy et al. 2011). Also, most of these studies
49 focused on the deterioration of the FRP and concrete bond rather than the behavior of the
50 FRP wrap under these harsh environments (Karbhari and Zhao 1998, Colombi et al. 2009,
51 Shi et al. 2013, Silva and Bicaia 2008, Yun and Wu 2011). Results from most studies
52 indicated that freeze-thaw cycling does not have a significant effect on the bond strength
53 between FRP and concrete and most of the specimens failed in the concrete substrate and not
54 along the bonded surface (Chajes et al. 1994, Colombi et al. 2009, Silva and Bicaia 2008,
55 Toutanji and El-Korchi 1999, Karbhari and Zhao 1998). However, one study found that the
56 failure was more brittle after freeze-thaw cycling (Karbhari and Zhao 1998).

57 A few studies reported the effect of harsh environment on FRP strength and the final
58 confined concrete strength of FRP-wrapped concrete specimens after exposure. Specimens
59 wrapped with CFRP experienced no reduction in strength or ductility due to wet-dry
60 exposure, whereas specimens wrapped with GFRP experienced more reduction in both
61 strength and ductility (Li and Karbhari 2003, Rivera and Karbhari and Zhao 1998, Toutanji
62 and Balaguru 1998, Steckel et al. 1998, Nardone et al. 2012). However, a study by Chin et al.
63 (1997) concluded that there was no significant reduction in the tensile strength of GFRP
64 when it was exposed to salt and distilled water for more than 1300 hours.

65 In a few studies the durability and strength of FRP-wrapped concrete columns under
66 simultaneous loading and environmental exposure was reported. Green et al. (2006) studied
67 the effect of sustained load and freeze-thaw cycles at the same time and concluded that

68 confined concrete strength was not reduced significantly for normal strength concrete.
69 However, there appears to be no research that investigated the simultaneous effect of freeze-
70 thaw cycling and corrosion of reinforcing bars. Usually corrosion of steel bars occurs due to
71 deicing salts, and the corrosion of steel bars and freeze thaw cycles can occur simultaneously.

72 In the research reported herein, a comprehensive experimental study was performed
73 to investigate the strength of FRP-wrapped cylinders when they were subjected to a sequence
74 of different environmental exposure conditions. First, the cylinders were subjected to
75 corrosion-like expansion and then to freeze-thaw conditioning. Corrosion-induced expansion
76 was simulated using the expanding cement Bristar. The expansion due to Bristar was
77 calibrated using experiments and validated using an analytical solution and finite element
78 analysis. Subsequently, the samples were subjected to 300 freeze-thaw cycles to study the
79 effect of both conditions on the compressive strength of the confined concrete.

80 **EXPERIMENTAL WORK**

81 **Durability of FRP Panel**

82 First the effect of freeze-thaw and wet-dry cycles on the durability of two different
83 types of FRP, glass FRP (GFRP) and carbon FRP (CFRP), was investigated. Four-ply GFRP
84 and two-ply CFRP sheets were fabricated using the wet lay-up process. The samples were
85 cured in air for 5 days according to vender recommendations. After curing, the FRP panels
86 were subjected to 300 freeze-thaw cycles. Subsequently, the FRP panels were cut into
87 coupons and strain gauges were mounted on the coupons. The width of the test specimens
88 varied from 13 to 19 mm (0.5 to 0.75 in.) and their length varied from 190 to 230 mm (7.5 to
89 9.0 in.), depending on the test. The gage length over which strains were measured was
90 89 mm (3.5 in.). The test machine was equipped with hydraulically actuated wedge grips

91 with serrated faces. The FRP coupons were tested under tension to determine the tensile
92 strength, f_u , ultimate strain, ϵ_u , and elastic modulus, E , of both the conditioned and
93 unconditioned sheets. All the tested coupons were selected from one GFRP panel and one
94 CFRP panel.

95 **Durability of Confined Concrete**

96 *Sample preparation:* After evaluation of the FRP panels, the effect of simultaneous
97 corrosion-like expansion and freeze-thaw cycles on the durability and strength of FRP-
98 wrapped concrete specimens was investigated. Ready mixed concrete with a water/cement
99 (w/c) ratio of 0.4 and an air entraining admixture was used. The 28-day mean compressive
100 strength of the concrete was 37.7 MPa (5,468 psi). A total of 30 specimens were cast. Two
101 different types of specimens were used; round cylinders with a diameter of 152 mm (6 in.)
102 and a height of 305 mm (12 in.), and square prisms with a 152 mm \times 152 mm cross section
103 and a 305 mm height. The corners of the square prisms were rounded to a 13 mm (0.5 in.)
104 radius. Since natural or accelerated corrosion tests are time consuming, an expanding cement
105 known as Bristar was used to simulate the expansion due to corrosion of reinforcing bars.
106 Out of 30 specimens, 24 specimens (12 round and 12 square), were fabricated with a 38 mm
107 (1.5 in.) diameter center hole in the longitudinal direction, and 6 specimens were cast as solid
108 round cylinders. The six solid round specimens without a center hole were not wrapped and
109 kept as control specimens. Solid square specimens without a center hole were not cast
110 because the strength of unwrapped concrete samples is not affected significantly by the
111 geometry of the cross section. The specimens with a center hole were wrapped with FRP and
112 then the center hole was filled with Bristar. The expansion force exerted by Bristar could be
113 controlled with the water to Bristar ratio and was calibrated using experiments, and analytical

114 and finite element modeling. Although steel rebars were not used, chloride was introduced
115 into the concrete by mixing 11 kg of NaCl/m³ of concrete, which translates to 2% Cl⁻ ions by
116 weight of cement (Arya and Said-Shawaqi 1996) during casting in order to simulate
117 contaminated concrete.

118 *Wrapping:* After 28 days of curing, out of a total of 24 wrapped specimens, 12 were
119 wrapped with three layers of GFRP and 12 with two layers of CFRP having fibers orientated
120 in the hoop direction. All wrapped specimens were subjected to expansion using Bristar one
121 week after wrapping.

122 *Freeze-Thaw:* After the initial expansion period of Bristar, which was about one
123 week, 15 specimens (12 wrapped and 3 unwrapped) were exposed to 300 freeze-thaw cycles
124 according to the ASTM C666 procedure and the other 15 samples were kept as control
125 specimens. Table 1 shows the number of samples in each batch.

126 *Strain Gauge Placement:* Strain gauges were used to monitor wrap hoop strains
127 during Bristar-induced expansion, and freeze-thaw and compression tests. Six round
128 specimens and six square specimens (three for each type of wrap) that were to undergo 300
129 cycles of freeze-thaw and four control specimen (one for each type of wrap and specimen
130 shape) were fitted with strain gauges. Each specimen was fitted with two strain gauges
131 oriented in the circumferential direction and placed opposite each other at mid-height. The
132 gauges were coated with wax and silicon to provide moisture and mechanical protection.

133 *Bristar:* The effectiveness of using Bristar to simulate corrosion-induced expansion
134 was initially tested on some trial specimens. The expansive nature of Bristar caused the trial
135 specimens to expand in the hoop direction as desired. However, an undesirable side effect
136 was the simultaneous expansion in the longitudinal direction. This caused the trial specimens

137 with the carbon wrap to split across a cross sectional plane since the carbon wrap contained
138 no longitudinal fibers. The glass wrap had bidirectional fibers and the fibers in the
139 longitudinal direction prevented the specimens from splitting. Additional longitudinal
140 reinforcement was provided to the carbon-wrapped test specimens by strengthening with
141 51 mm (2 in.) wide strips of carbon in the longitudinal direction. The strips were spaced with
142 51 mm (2 in.) gaps between them around the circumference. The strain gauge readings were
143 not affected because the strips were placed adjacent to the gauges and the longitudinal strips
144 did not provide any additional lateral confinement.

145 **BRISTAR CALIBRATION**

146 The Bristar mix was used to simulate the internal pressure applied by corroding
147 reinforcing bars. The amount Bistar expands is highly dependent on the water to Bristar ratio.
148 An attempt was made to calibrate the water/Bristar ratio so that a confining pressure in the
149 FRP wraps similar to that developed by corrosion-induced expansion could be generated.
150 Experimental testing was initially performed and then analytical calculations were conducted
151 to calibrate the internal pressure of Bristar expansion to match the pressure due to corrosion
152 of steel bars resulting from a 33% mass loss reported by Harichandran and Baiyasi (2000).
153 Later, the results were validated using finite element simulations.

154 **Experimental Testing**

155 Two concrete specimens to be used for calibration were cast in 4.77 mm thick steel
156 tubes having the same dimensions of a 152 mm diameter, 305 mm height, and a 38 mm
157 center hole. Strain gauges were mounted on the steel tube to monitor its hoop strain. After the
158 concrete was allowed to cure for 28 days, Bristar was prepared with the two different
159 water/Bristar ratios of 0.4 and 0.5 and was poured into the center hole. The strains developed

160 in the steel tubes were monitored for 9-13 days until Bristar reached its final volume and the
161 strains stabilized. Figure 1 shows the strain developed in the steel tube in the calibration
162 samples. The strain in the steel tube reached 380 microstrains ($\mu\epsilon$) in about 4 days for the
163 water/Bristar ratio of 0.5 and around 660 $\mu\epsilon$ in about 7 days for the water/Bristar ratio of 0.4.

164 **Analytical Method**

165 From the mechanics of thin walled cylinders, the confining pressure in a confined
166 column is given by

$$167 \quad f_r = \frac{2(E \epsilon_t t n)}{D} \quad (1)$$

168 where t = thickness of the steel tube or wrap per layer, ϵ_t = circumferential strain of the tube,
169 E = elastic modulus of the tube, n = number of FRP or steel tube layers and D = diameter of
170 the cylindrical column.

171 Using Equation 1, the confining pressures in the steel tube were estimated from the
172 maximum hoop strain in the steel tube shown in Figure 1 for the two different water/Bristar
173 ratios. The maximum confining pressures calculated using Equation 1 were 4.76 MPa
174 (690 psi) and 8.27 MPa (1200 psi) for water/Bristar ratios of 0.5 and 0.4, respectively, and
175 are shown in Table 2. Assuming that the same confining pressures would be developed if
176 three layers of GFRP wrap confined the specimens instead of the steel tube, the hoop strains
177 in the GFRP wrap were back calculated using Equation 1. The hoop strain in a 3-layer GFRP
178 wrap that would induce the confining pressures of 4.76 and 8.27 MPa were estimated to be
179 4,500 $\mu\epsilon$ and 7,800 $\mu\epsilon$, respectively. These hoop strains were compared with those in a 3-
180 layer GFRP wrap reported by Harichandran and Baiyasi (2000) for a 33% mass loss resulting
181 from accelerated corrosion for 190 days. Harichandran and Baiyasi studied the effect of

182 bonded and unbonded FRP wraps on the corrosion rate and used 152 mm diameter and
183 305 mm high concrete cylindrical specimens (the same as the calibration specimens in this
184 study), with four #13 steel reinforcing bars placed with 13 mm of cover. They used two bars
185 as anodes and two bars as cathodes to keep the corrosion products within the specimens as in
186 natural corrosion. Figure 2 shows the GFRP strains reported by Harichandran and Baiyasi
187 (2000) for one specimen. The strain gauge was located at the crack location and yielded a
188 strain of about 4,000 $\mu\epsilon$. Comparing this strain with the GFRP wrap hoop strains of 4,500 $\mu\epsilon$
189 and 7,800 $\mu\epsilon$ for the water/Bristar ratios of 0.4 and 0.5, respectively, calculated from
190 Equation 1, the water/Bristar ratio of 0.5 appeared appropriate for the experimental study.

191 **Numerical Validation**

192 The analytical model assumes that the expanding Bristar causes the same confining
193 pressure to be applied by the steel tube and GFRP wrap. This assumption is inaccurate
194 because the stiffness of steel and GFRP is different. The GFRP wrap will expand more than
195 the steel tube resulting in a lower confining pressure. A finite element model can capture this
196 behavior and was used to verify whether the water/Bristar ratio of 0.5 was indeed appropriate
197 for the experimental study.

198 The general-purpose FE program ABAQUS (Version 6.12) was used. First, an FE
199 model of the calibration specimen with the steel tube and the center hole was analyzed. In the
200 FE analysis, a uniform radial pressure was applied to the inside surfaces of the center hole of
201 the round calibration specimens to simulate the pressure exerted by expanding Bristar. Since
202 the round calibration specimens were radially symmetric, only one quarter of the specimens
203 was modeled in the FE analysis and appropriate boundary conditions were applied (i.e., free
204 movement of boundary nodes in the radial and longitudinal directions). The insets in Figures

205 3 and 4 show the finite element meshes used. The material models used in ABAQUS are
206 described below.

207 *Concrete:* The Drucker-Prager plasticity model in ABAQUS was used to model the
208 behavior of the confined concrete. The main parameters of the model, such as dilation and
209 friction angles, were selected from the literature (Yu et al, 2010). Other parameters of the
210 model included the concrete compressive strength and elastic modulus, which were obtained
211 through laboratory testing and the ACI equation (i.e., $E_c = 4700\sqrt{f'_c}$ MPa), respectively,
212 and are listed in Table 3.

213 *Steel Reinforcement:* The steel tube in the calibration specimen was modeled as an
214 isotropic elastic-perfectly plastic material. The parameters required for the material model
215 were elastic modulus, yield strength and Poisson's ratio, and the values selected from the
216 literature are shown in Table 3.

217 *FRP Material:* The orthotropic linear elastic material model with the Lamina option
218 was used to model the GFRP wrap used by Harichandran and Baiyasi (2000) in their
219 accelerated corrosion test specimens. Model parameters such as the elastic and shear moduli
220 in all directions and Poisson's ratio were selected based on the mechanical properties
221 provided by the manufacturer and are shown in Table 3.

222 *Concrete Interface:* The interfaces between the concrete/steel tube and
223 concrete/GFRP wrap were assumed to be fully bonded. Full bonding between the surfaces
224 was achieved by using the tie option in ABAQUS.

225 The internal radial pressures that caused the same hoop strains in the steel tube as in
226 the experimental specimens for the water/Bristar ratios of 0.4 and 0.5 were estimated.
227 Figure 3 shows how the strain in the steel tube in the FE model of the calibration specimens

228 changes with the radial pressure applied to the inside of the center hole. The pressures
229 causing strains of $380 \mu\epsilon$ and $660 \mu\epsilon$ in the steel tube were estimated to be 22 MPa and
230 25.5 MPa, respectively. These pressures correspond to those that Bristar with water/Bristar
231 ratios of 0.5 and 0.4 applies to the surrounding concrete in the calibration specimens,
232 respectively. These pressures were then applied in the FE model of the calibration specimens
233 with three layers of GFRP wrap and the strains in the wrap were compared with the strain of
234 about $4,000 \mu\epsilon$ measured in the GFRP wrap by Harichandran and Baiyasi (2000). Figure 4
235 shows the relationship between the internal radial pressure and the GFRP wrap strain in the
236 FE simulations. The strains in the GFRP wrap due to the internal radial pressures of 22 MPa
237 (corresponding to water/Bristar ratio of 0.5) and 25.5 MPa (corresponding to a water/Bristar
238 ratio of 0.4) were $3,800 \mu\epsilon$ and $5,000 \mu\epsilon$, respectively. As expected, the analytical model was
239 inaccurate and the hoop strains in the GFRP wrap from finite element simulations are lower
240 than those computed by the analytical method. Nevertheless, the FE analysis confirms that
241 the water/Bristar ratio of 0.5 is appropriate to simulate corrosion-induced expansion because
242 the predicted GFRP strain of $3800 \mu\epsilon$ is close to the peak strain of $4,000 \mu\epsilon$ measured by
243 Harichanandran and Baiyasi (2000) for 33% of mass loss in their accelerated corrosion test.

244

245

RESULTS AND DISCUSSION

246 Durability of FRP Panel

247 Table 4 lists the mechanical properties of the FRP panels before and after freeze-thaw
248 exposure. Note that different sets of specimens were used for the unconditioned modulus and
249 strength tests. It was difficult to control the thickness of panels fabricated using the wet lay-
250 up process and the mechanical properties of the FRP panels are sensitive to specimen

251 thicknesses. To avoid this sensitivity, the effective stiffness (i.e., modulus \times thickness) and
252 ultimate strength per unit width (i.e., ultimate strength \times thickness) were used to compare
253 results.

254 Figure 5 and Table 4 indicate that freeze-thaw conditioning had little effect on the
255 mean effective stiffness of glass panels, while for carbon panels it appears to have increased
256 by 30%, the latter being significant at the 95% level. The decrease of 21% in the mean
257 ultimate strength per unit width of glass is significant at the 95% level, but the apparent
258 increase in strength for carbon is not significant at the 95% level (because of the large
259 variation for the unconditioned panels). The decrease of 20% and 28% in the mean ultimate
260 strains of glass and carbon panels, respectively, is significant at the 95% confidence level. It
261 should be noted that many of the failures occurred at the grips and may have been premature.
262 The ultimate strains of the unconditioned and conditioned specimens are significantly lower
263 than the values reported by the manufacturer.

264 **Durability of Confined Concrete**

265 Strength and durability tests were performed on FRP-wrapped round and square
266 cylinders. The primary purpose of the tests was to determine the durability of the FRP tubes
267 under simultaneous corrosion and freeze-thaw cycling, with strength considerations being
268 secondary.

269 *Corrosion expansion:* Initially, the expansion due to accelerated corrosion for 190
270 days causing 33% mass loss was simulated using Bristar. Based on the calibration results
271 reported earlier, the water/Bristar ratio was selected to be 0.5.

272 Initial strain gauge readings from the FRP wrap were taken prior to pouring Bristar in
273 the center hole of each specimen. Since Bristar is highly porous and water absorption with

274 subsequent freezing and thawing within the hole containing Bristar was undesirable, the ends
275 of the specimens were coated with epoxy prior to the freeze-thaw tests after the Bristar had
276 fully expanded.

277 The average strain in the wraps after adding Bristar varied from 3,100 to 6,000 $\mu\epsilon$ for
278 GFRP-wrapped specimens with an average of 4,700 $\mu\epsilon$ and 2,400 to 6,800 $\mu\epsilon$ for CFRP-
279 wrapped specimens with an average of 4,800 $\mu\epsilon$. Variations in these values occurred because
280 it was not possible to control the pressure exerted by Bristar precisely. However, the average
281 strain values were a little higher than the strain of 4,000 $\mu\epsilon$ measured by Harichandran and
282 Baiyasi (2000) in the GFRP wrap due to steel corrosion and 33% mass loss (see Figure 2)
283 and the predictions of 4,500 $\mu\epsilon$ and 3,800 $\mu\epsilon$ from the analytical and FE models. As shown in
284 Figures 6a and 6b, the round specimens had lower strains (average of 3200 $\mu\epsilon$) that were
285 closer to the FE predictions compared to the square specimens because the Bristar calibration
286 was done using round specimens.

287 *Freeze-Thaw Test:* After corrosion-like expansion of wrapped specimens, they were
288 subjected to freeze-thaw cycles according to the ASTM C666 Procedure B, with freezing in
289 air and thawing in water. Thermocouples mounted at the center of wrapped and unwrapped
290 control specimens were used to measure the internal temperatures during testing. Since the
291 wrapped specimens took longer to reach -17.8°C (end set point for the freeze cycle) and
292 4.4°C (end set point for the thaw cycle) than the unwrapped specimens, the freeze-thaw
293 machine was precisely calibrated before the test. ASTM C666 allows a tolerance of $\pm 1.7^{\circ}\text{C}$ at
294 the upper and lower set points. By adjusting the sump water temperature during a few trial
295 cycles, it was determined that a sump water temperature of 7.2°C would ensure that all

296 specimens attained temperatures of $-17.78 \pm 1.7^\circ\text{C}$ at the end of the freeze cycle and
297 $4.4 \pm 1.7^\circ\text{C}$ at the end of the thaw cycle and thereby the test conformed to ASTM C666.

298 The FRP hoop strains were monitored twice a day during the entire testing period for
299 specimens fitted with strain gauges. Two readings were made each day, one during the freeze
300 phase and the other during the thaw phase. The strains were measured throughout this period.
301 All strain gauges survived the freeze-thaw test. Figures 6a and 6b show the strain in the FRP
302 wraps during the freeze-thaw cycles for GFRP and CFRP, respectively. In general, the strain
303 during the freeze cycle was 100-200 $\mu\epsilon$ higher than that during the thaw cycle. This is most
304 likely due to the thermal contraction of the glass wrap during freezing. However, for carbon
305 there was only a slight difference between thaw and freeze readings since its coefficient of
306 thermal expansion is close to zero.

307 *Compression Test:* Figure 7 and Table 5 show results of the compression tests for round
308 and square wrapped specimens without and with freeze-thaw conditioning. All the FRP-
309 wrapped specimens were subjected to corrosion-like expansion simulated with Bristar, all
310 conditioned specimens were subjected to 300 cycles of freeze-thaw cycles, and control
311 specimens were not subjected to freeze-thaw cycles. None of the plain concrete specimens
312 were subjected to corrosion-like expansion simulated by Bristar. The following observations
313 are made:

- 314 • **Plain round specimens:** Only one of three specimens survived freeze-thaw conditioning
315 for 300 cycles. The two specimens that did not survive had extensive cracking and
316 spalling due to freeze-thaw cycles, which made it impossible to perform compression
317 testing on them. The specimen that survived had approximately the same compression

318 strength as the control specimens (~35-45 MPa). There was no significant reduction in
319 strength due to freeze-thaw conditioning if the specimen survived.

320 • **Round glass-wrapped specimens:** In general, conditioning had little effect and the
321 compression strength was approximately the same for control and conditioned specimens.
322 The strength of wrapped specimens (~105-110 MPa) was approximately 2.6 times larger
323 than the strength of unwrapped specimens.

324 • **Round carbon-wrapped specimens:** Conditioning reduced the compression strength
325 from about 95 MPa to about 80-94 MPa, generally representing about a 15% strength
326 loss. The strength of wrapped specimens (~95 MPa) was approximately 2.3 times larger
327 than the strength of unwrapped specimens.

328 • **Square glass-wrapped specimens:** Again, conditioning had little effect on the
329 compressive strength (~62-66 MPa). The strength of wrapped specimens was
330 approximately 1.5 times larger than the strength of unwrapped specimens.

331 • **Square carbon-wrapped specimens:** Conditioning reduced the compression strength
332 slightly from about 58-65 MPa to about 55-63 MPa. The strength of wrapped specimens
333 (~60 MPa) was approximately 1.4 times larger than the strength of unwrapped
334 specimens.

335 The wrapped square prisms had lower compressive strength compared to the wrapped
336 round cylinders, even though the cross sectional area of the prisms was higher than that of
337 the cylinders. This was due to the reduced confinement provided by the wraps for square
338 cross sections and stress concentrations that develop at the corners. For square prisms, glass
339 and carbon wraps increased the strength by about the same amount. Wrapped square prisms
340 always failed by rupture of the wrap at a corner. A reduction in compression strength of

341 approximately 30-40% was observed between the round cylinders and the square prisms. The
342 wrapped square prisms also demonstrated a sudden loss of strength after the peak stress was
343 reached. However, the wraps were undamaged during this loss of strength. The loss of
344 strength was most likely due to the failure of the ineffectively confined regions of concrete.
345 These regions do not experience capacity enhancement due to poor confinement.

346 Table 5 shows the mean ultimate compression strengths and 95% confidence margins
347 for each category of specimens. The cross sectional area lost by the cavity containing Bristar
348 was deducted when calculating the strengths. At the 95% confidence level, means of the
349 compressive strength of specimens subjected to freeze-thaw cycles are not significantly
350 different from those of control specimens. Similarly, the freeze-thaw cycles have no
351 statistically significant effect on the compressive strength of square prisms. The reduction in
352 mean compressive strength observed for carbon-wrapped specimens after freeze-thaw
353 conditioning is not statistically significant for the sample size used in this study.

354

355 **SUMMARY AND CONCLUSIONS**

356 Strength and durability tests were carried out on round cylinders and square prisms
357 made of concrete and wrapped with glass and carbon FRP. An expanding cement known as
358 Bristar was used in the wrapped specimens to investigate the durability of glass and carbon
359 wraps under sustained expansion load and subjected to freeze-thaw cycling. The sustained
360 expansion load simulated the load generated in wrapped columns by corrosion products.
361 Chloride was impregnated into the cylinders during casting in order to simulate concrete
362 exposed to salt. The compression strength of plain control cylinders as well as wrapped test

363 specimens after 300 cycles of freeze-thaw conditioning was measured. A total of 60
364 specimens were used in the freeze-thaw test.

365 The means of the compressive strength of freeze thaw specimens were not
366 significantly different from those of control specimens at the 95% confidence level. This was
367 true both for carbon and glass wraps, and for specimens with round and square cross
368 sections. The results indicate that the wraps did not sustain significant damage due to freeze-
369 thaw cycling under sustained load.

370 The wrapped square prisms had lower compressive strengths compared to the
371 wrapped round cylinders, even though the cross sectional area of the square prisms was
372 higher than that of the round cylinders. This was due to the reduced confinement provided by
373 the wraps for square cross sections and stress concentrations that develop at the corners.
374 Wrapped square prisms always failed by rupture of the wrap at a corner. A reduction in the
375 failure strength of approximately 30-40% was observed for the square specimens compared
376 to the round specimens.

377 The compression strength of wrapped specimens was 1.4 to 2.6 times larger than that
378 of unwrapped specimens for square and round cross sections, respectively.

379

380 **ACKNOWLEDGEMENTS**

381 This research was sponsored by the Michigan Department of Transportation.

382

383 **REFERENCES**

384 Almusallam, T. H., Al-Salloume, Y. A., and Alsayed, S. H. (2000). "Durability of concrete
385 cylinders wrapped with GFRP sheets at different environmental conditioning." *Seventh*

386 *Annual International Conference on Composites Engineering*, Denver, Colorado, July 2-
387 8, 27-28.
388
389 Arya, C., and Sa'id-Shawqi, Q. (1996). "Factors influencing electrochemical removal of
390 chloride from concrete." *Cement and Concrete Research*, 26(6), 851-860.
391
392
393 Chajes, M.J., Mertz, D.R., and Thomson, T.A. (1994). "Durability of composite material
394 reinforcement." *Proceedings, Third Materials Engineering Conference*, ASCE, San
395 Diego, California.
396
397 Chin, J. W., Nguyen, T., and Aouadi, K. (1997). "Effects of environmental exposure on
398 fiber-reinforced plastic (FRP) materials used in construction." *Journal of Composites*
399 *Technology and Research*, 19(4), 205-213,
400
401 Colombi, P., Fava, G. and Poggi, C., (2010). "Bond strength of CFRP-concrete elements
402 under freeze-thaw cycles." *Composite Structures*, 92(4), 973-983.
403
404 Du, Y. G., Chan, A. H. C., and Clark, L.A (2006). "Finite element analysis of the effects of
405 radial expansion of corroded reinforcement." *Computers and Structures*, 84(13-14), 917-
406 929.
407
408 El-Zefzafy, H., Mohamed, H. M., and Masmoudi, R. (2011). "Freeze-thaw effects on the
409 behavior of concrete-filled FRP tube columns." *Proceedings, Annual Conference of the*
410 *Canadian Society for Civil Engineering*, 2, 1563-1572.
411
412 Gomez, J., and Casto, B. (1996). "Freeze-thaw durability of composite materials."
413 *Proceedings, 1st International Conference on Composites in Infrastructure (ICCI)*,
414 Tucson, AZ, 947-955.
415
416 Green, M. F., Bisby, L. A., Fam, A. Z., and Kodur, V. K. (2006). "FRP confined concrete
417 columns: behaviour under extreme conditions." *Cement and Concrete Composites*,
418 28(10), 928-937.
419
420 Harichandran, R. S., and Baiyasi, M. I. (2000). "Repair of corrosion-damaged columns using
421 FRP wraps." *Report No. RC-1386*, Michigan Department of Transportation, Lansing,
422 Michigan.
423
424 Karbhari, V. M. and Zhao, L., (1998). "Issues related to composite plating and environmental
425 exposure effects on composite-concrete interface in external strengthening." *Composite*
426 *Structures*, 40(3/4), 293-304.
427
428 Li, Y., and Karbhari, V. M. (2003). "Durability characterization of T700 based composites
429 for use in civil infrastructure." *Proceedings, 44th International SAMPE Symposium and*
430 *Exhibition, Vol. II*, 1540-1552.

431
432 Mehta, P., and Monteiro, J. (1993). *Concrete, structure, properties, and materials*. Second
433 Edition, Prentice-Hall, Englewood Cliffs, 160-164.
434
435 Nardone, F., Di Ludovico, M., De Caso Y., Basalo, F. J., Prota, A., and Nanni, A. (2012).
436 “Tensile behavior of epoxy based FRP composites under extreme service conditions.”
437 *Composites Part B: Engineering*, 43(3), 1468-1474.
438
439 Rivera, J., and Karbhari, V. (1999). “Effects of extended freeze-thaw exposure on composite
440 wrapped concrete cylinders.” *Proceedings*, 44th SAMPE Symposium, Long Beach,
441 California, May 23-27.
442
443 Shi, J., Zhu, H., Wu, Z., Seracino, R., and Wu, G. (2013). ”Bond behavior between basalt
444 fiber–reinforced polymer sheet and concrete substrate under the coupled effects of freeze-
445 thaw cycling and sustained load.” *Composites in Construction*, 17(4), 530-542.
446
447 Silva, M. A. G, and Biscaia, H. (2008). “Degradation of bond between FRP and RC beams.”
448 *Composite Structures*, 85(2), 164-174.
449
450 Soudki, K. A. (1997). “Freeze-thaw response of CFRP wrapped concrete.” *Concrete*
451 *International*, 19(8), 64-67.
452
453 Steckel, G. L., Hawkins, G. F., and Bauer, J. L. (1998). “Environmental durability of
454 composites for seismic retrofit of bridge columns.” *2nd International Conference on*
455 *Fiber Composites in Infrastructure ICCI*, Vol.2, Tucson, 460–475.
456
457 Toutanji, H., and Balaguru, P. (1998). “Durability characteristics of concrete columns
458 wrapped with FRP tow sheets.” *Journal of Materials in Civil Engineering*, 10(1), 52-57.
459
460 Toutanji, H., and El-Korchi, T. (1999). “Tensile durability of cement-based FRP composite
461 wrapped specimens.” *Journal of Composites for Construction*, ASCE, 3(1), 38-45.
462
463 Yu, T., Teng, J. G., Wong, Y. L., and Dong, S. L. (2010). “Finite element modeling of
464 confined concrete-I: Drucker-Prager type plasticity model.” *Engineering Structures*,
465 32(3), 665-679.
466
467 Yun, Y., and Wu, Y. F. (2011). “Durability of CFRP-concrete joints under freeze-thaw
468 cycling.” *Cold Reg. Sci. Technol.*, 65(3), 401–412.
469
470

471
472

Table 1: Freeze-Thaw Laboratory Testing Matrix

Specimen Type	Conditioning	No. of Specimens		
		Unwrapped	GFRP	CFRP
Round Square	None	3	3 3	3 3
Round Square	300 cycles of freeze-thaw	3	3 3	3 3

473
474

475
476
477
478
479
480
481
482
483
484

Table 2: Analytical Estimate of Maximum Confining Pressure and GFRP Strain

Water/Bristar Ratio	Measured Strain ($\mu\epsilon$)	Confining Pressure (MPa)	Strain in GFRP ($\mu\epsilon$)
0.5	380	4.76	4500
0.4	660	8.27	7800

485
486
487
488
489
490
491
492
493
494
495

Table 3: Parameters used in FE Analysis

Materials	Elastic Modulus (GPa)	Strength (MPa)	Thickness (mm)	Poisson's Ratio
Concrete	28.8	(Compressive) 37.7	NA	0.16
Steel	200.0	410.0	4.77	0.3
GFRP	(Fiber direction) 27.6	NA	1.00	0.29

496

Table 4: Mechanical Properties of FRP Panels Before and After Freeze-Thaw Exposure

Wrap Type	Thickness (mm)	Modulus (MPa)	Effective Stiffness (N/mm)	Ultimate Strength per Unit Width (N/mm)	Ultimate Strain
		No Exposure			
GFRP	1.227	22,011	27,000	536	0.02
CFRP	0.625	53,061	33,150	415	0.015
		300 Freeze-Thaw Cycles			
GFRP	1.092	23,805	26,000	424	0.016
CFRP	0.508	79,012	40,138	448	0.01

497

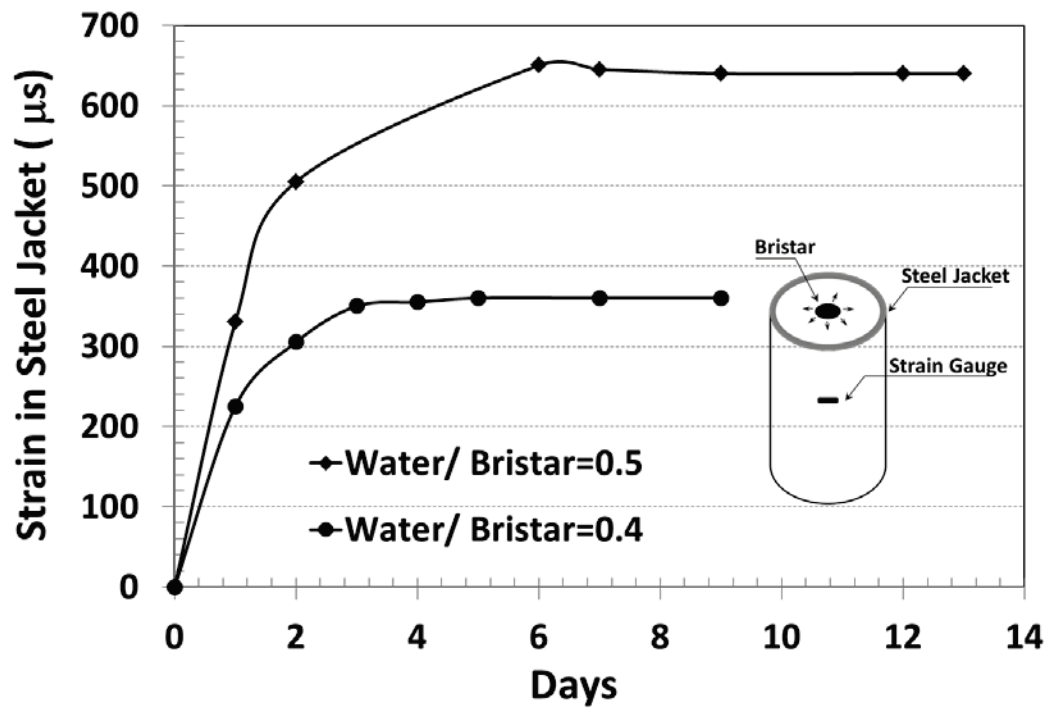
498

499

Table 5: Compression Test Summary Data

Specimens Type			Ultimate Compressive Strength (kPa)		
Wrap	Shape	Condition	Average	Standard Deviation	95% Conf. Margin
No Wrap	Round	Control	41,074	2,531	±2,656
		F/T	42,875	NA	NA
GFRP	Square	Control	63,601	1,907	±2,002
		F/T	63,761	1,208	±3,002
	Round	Control	109,911	3,856	±6,136
		F/T	108,370	1,727	±4,291
CFRP	Square	Control	91,924	2,652	±2,783
		F/T	59,384	3,149	±7,822
	Round	Control	92,558	3,612	±3,791
		F/T	84,714	8,440	±20,967

500
 501
 502
 503
 504
 505
 506
 507
 508
 509
 510
 511
 512
 513



514
 515
 516
 517
 518
 519
 520
 521
 522

Figure 1: Strain in steel tube for different water to Bristar ratios

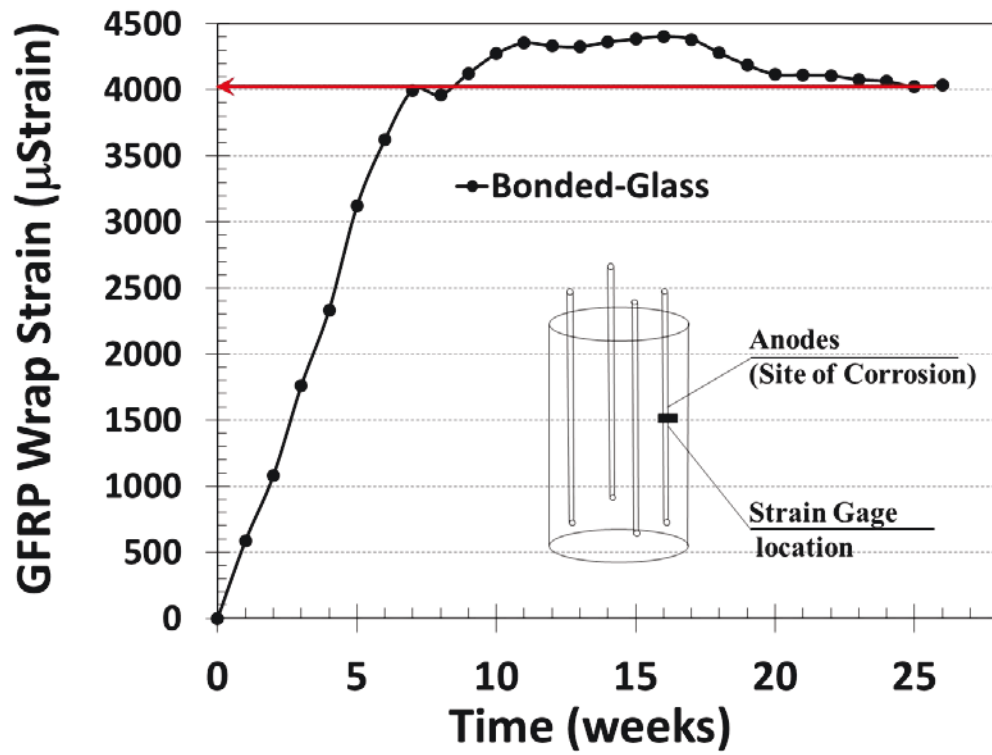


Figure 2: Strain developed in GFRP wrap in accelerated corrosion test (Harichandran and Baiyasi 2000)

523
 524
 525
 526
 527
 528
 529
 530
 531
 532
 533
 534
 535
 536
 537
 538
 539
 540
 541
 542
 543

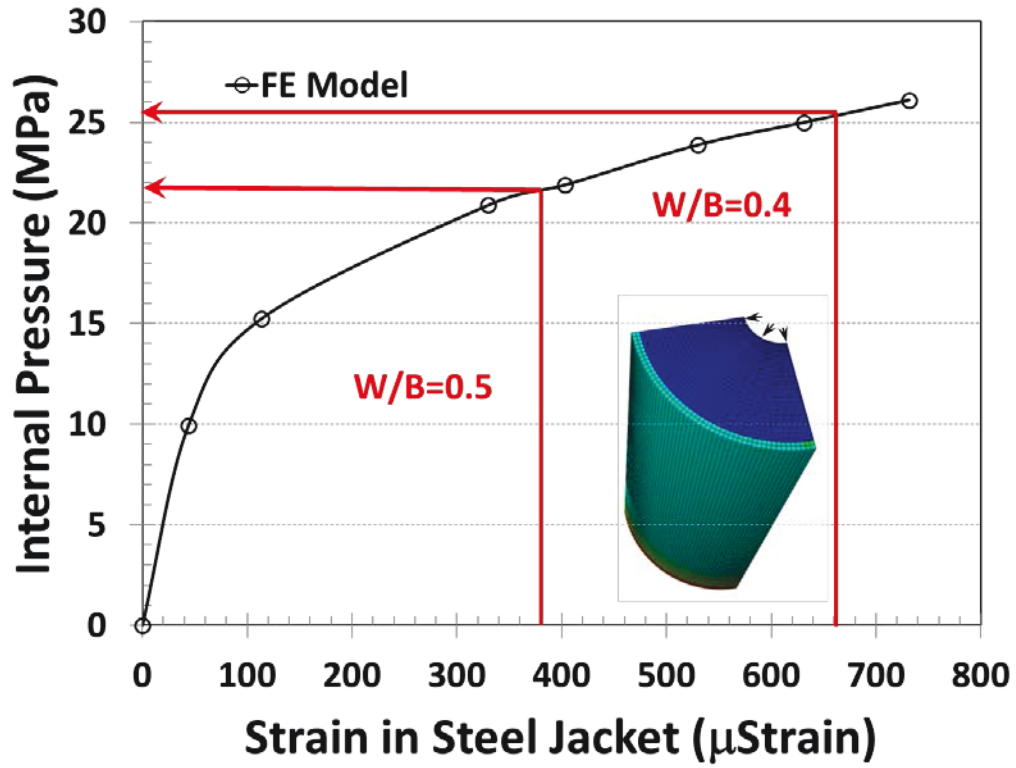


Figure 3: Strain developed in steel tube in FE model of calibration specimens

544
 545
 546
 547
 548
 549
 550
 551
 552
 553
 554
 555
 556
 557
 558
 559
 560
 561
 562
 563
 564
 565
 566
 567
 568

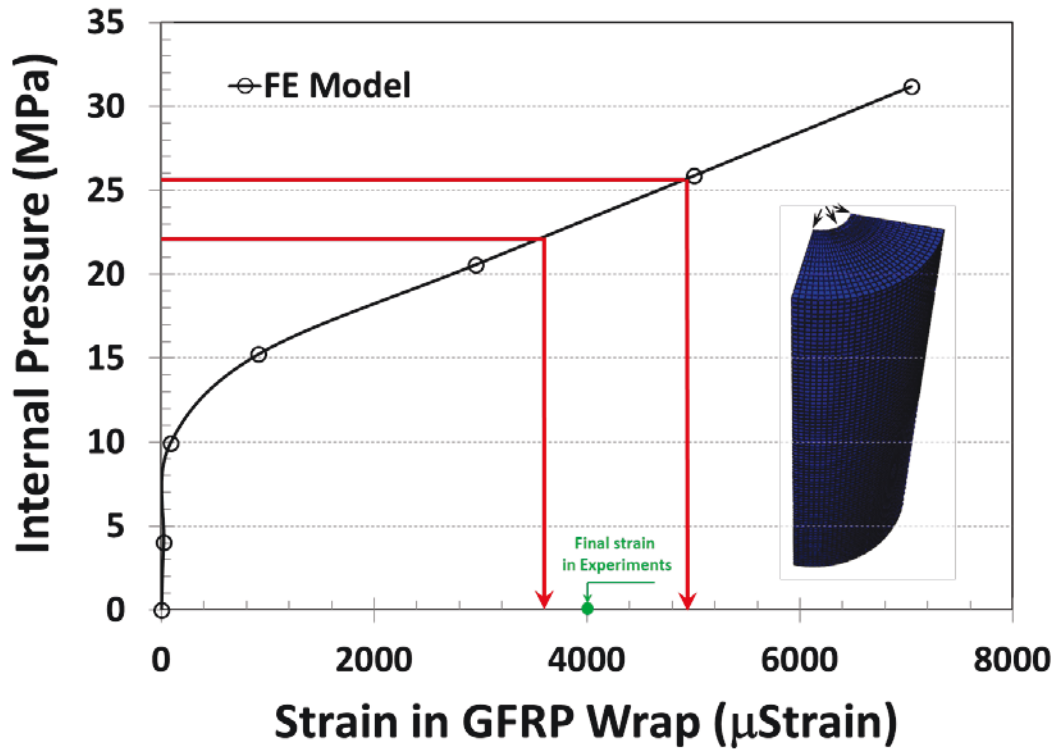


Figure 4: Strain developed in GFRP wrap in FE model of test specimens

569
 570
 571
 572
 573
 574
 575
 576
 577
 578
 579
 580
 581
 582
 583
 584
 585
 586
 587
 588
 589
 590
 591
 592
 593

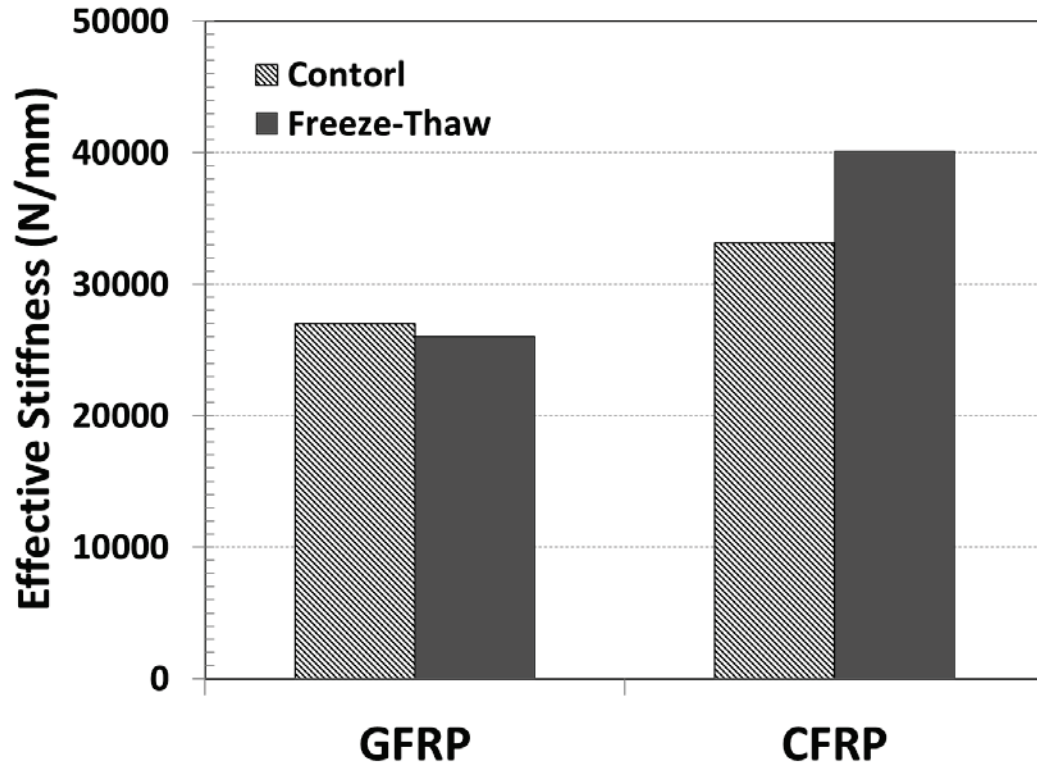
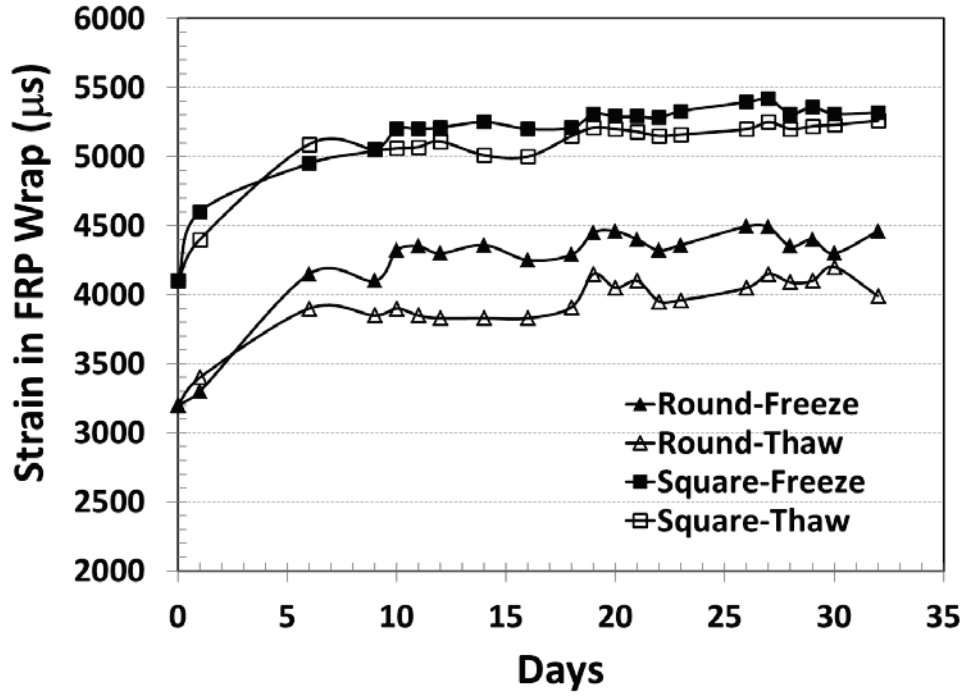


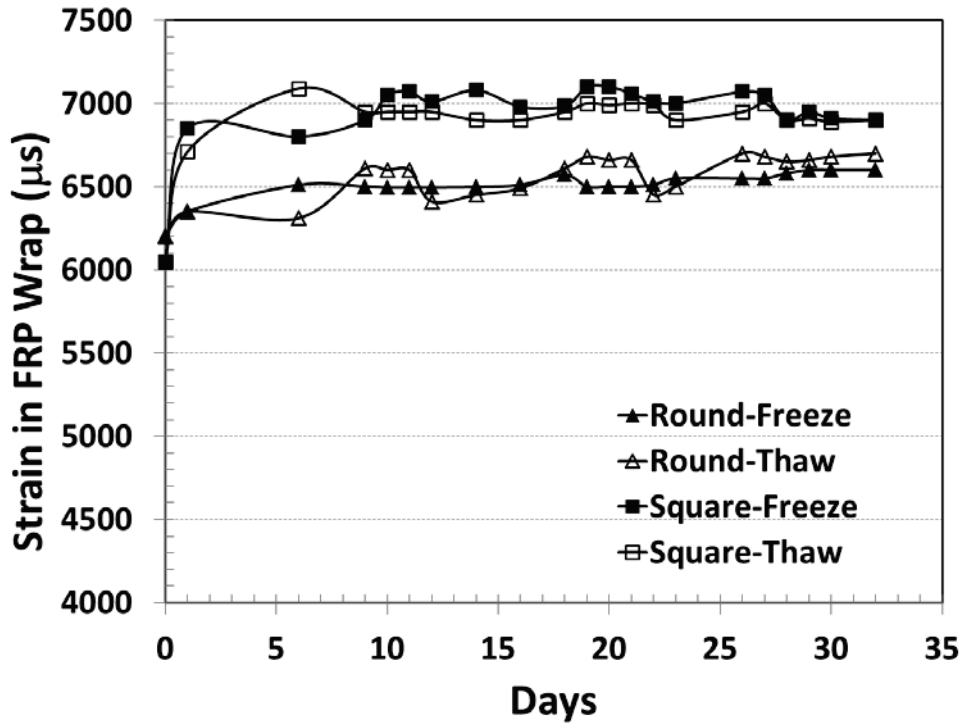
Figure 5: Effective stiffness of FRP panels after 300 freeze-thaw cycles

594
 595
 596
 597
 598
 599
 600
 601
 602
 603
 604
 605
 606
 607
 608
 609
 610
 611
 612
 613
 614
 615
 616
 617



618
619
620

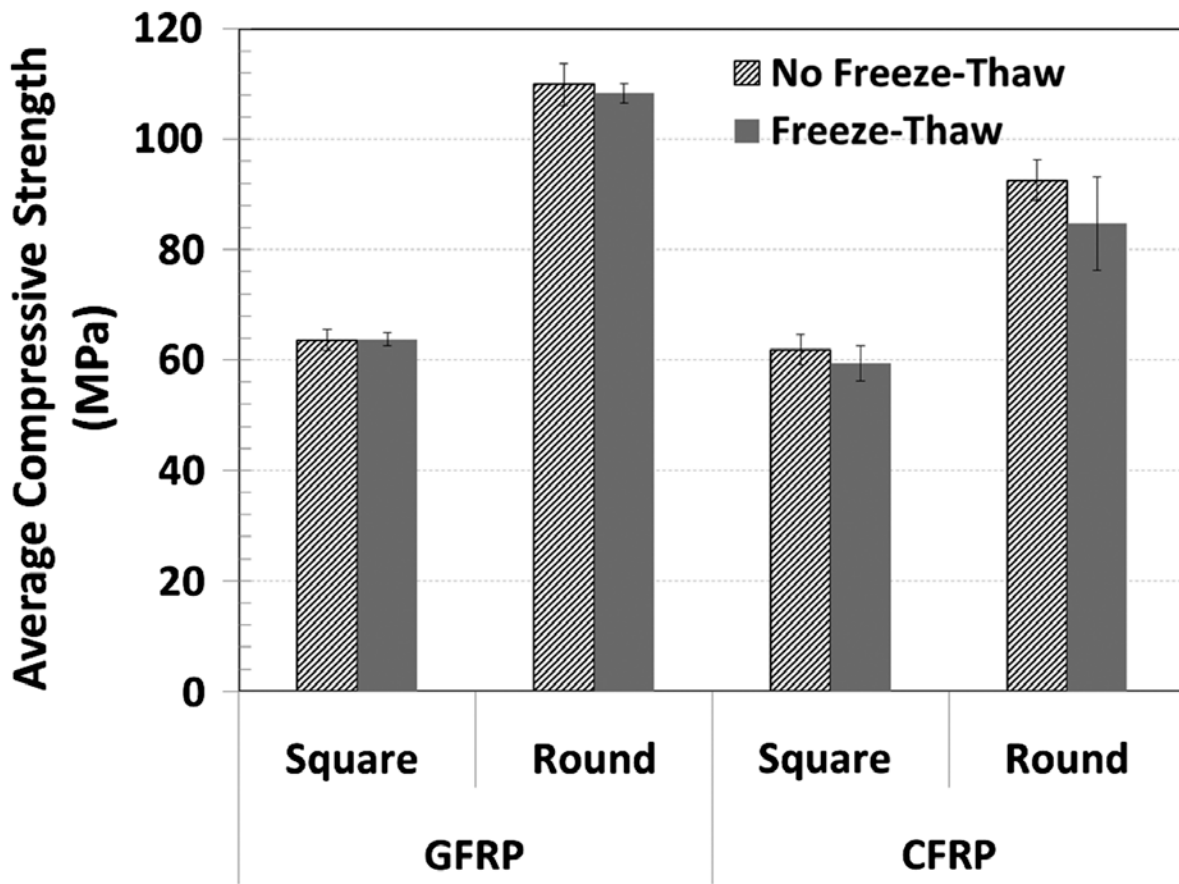
(a)



621
622
623
624
625

(b)

Figure 6: Strain in FRP wrap during freeze-thaw cycles (a) glass, (b) carbon



627
628
629
630
631

Figure 7: Results of the compression tests for round and square wrapped specimens